

2 **QUADICA v2: Extending the large-sample data set for water**
3 **QUAlity, DIcharge and Catchment Attributes in Germany**

4
5 Pia Ebeling¹,
6 Alexander Hubig¹,
7 Alexander Wachholz³,
8 Ulrike Scharfenberger⁴,
9 Sarah Haug¹,
10 Tam Nguyen¹,
11 Fanny Sarrazin⁵,
12 Masooma Batool²,
13 Andreas Musolff¹,
14 Rohini Kumar²
15

16 ¹Department of Hydrogeology, Helmholtz Centre for Environmental Research-UFZ, Leipzig, 04318,
17 Germany

18 ²Department of Computational Hydrosystems, Helmholtz Centre for Environmental Research-UFZ,
19 Leipzig, 04318, Germany

20 ³Department of Inland Surface Waters, German Environment Agency-UBA, Dessau, 06844, Germany

21 ⁴Department Aquatic Ecosystems Analysis and Management, Helmholtz Centre for Environmental
22 Research-UFZ, Magdeburg, 39114, Germany

23 ⁵Université Paris-Saclay, INRAE, UR HYCAR, 92160 Antony, France

24 *Correspondence to:* Pia Ebeling (pia.ebeling@ufz.de)

27 **Abstract**

28 The QUADICA version 2 dataset significantly expands upon the first version of QUADICA (water
29 QUAlity, DIcharge and Catchment Attributes for large-sample studies in Germany), by incorporating
30 more recent data, additional water quality and driver variables, and more stations with concurrent water
31 quantity data. Specifically, QUADICA v2 extends the water quality time series of the first version up to
32 2020 and introduces new variables, including water temperature, oxygen, and chlorophyll-a
33 concentrations, as well as concentrations of ammonium, sulfate, and geogenic solutes like calcium. These
34 additions enable a more comprehensive understanding of ecological impacts, including eutrophication
35 effects, and water quality dynamics across catchments. Furthermore, the number of stations with both
36 water quality and quantity data has effectively doubled – now covering 637 out of the total 1386 stations
37 – by integrating QUADICA with the CAMELS-DE and Caravan-DE datasets. The inclusion of time series
38 on point and diffuse sources of both nitrogen and phosphorus allows for more thorough investigations of
39 driver-response relationships and nutrient export from catchments. To facilitate visualization and
40 exploration of QUADICA, we provide a user-friendly, interactive R application alongside the online data
41 repository, as well as a browser-based web app for inspecting the dataset. This makes QUADICA v2 a
42 comprehensive dataset that spans from driver to impact variables, offering a valuable resource for
43 researchers and practitioners.

44

45 **1 Introduction**

46 High water quality is critical for the health of aquatic ecosystems and humans. Understanding the spatial
47 and temporal variability in water quality variables is essential for effective management and conservation
48 of water resources. Observational data are the key to propelling our understanding of hydrological and
49 biogeochemical processes and complex interactions. Large-sample hydrology (LSH) addresses the “need
50 to balance depth and breadth” (Gupta et al., 2014) and has thus become a cornerstone to understand the
51 generality of patterns and processes across diverse landscape and climate settings.

52 LSH data sets that combine stream observations with contextual data on catchment attributes and driving
53 forces have gained momentum in recent years. For water quantity, the CAMELS data sets available in
54 several countries (Addor et al., 2017; Alvarez-Garreton et al., 2018; Coxon et al., 2020; Chagas et al.,
55 2020; Fowler et al., 2021; Loritz et al., 2024) and the globally consistent data set Caravan (Kratzert et al.,
56 2023) are prominent examples. For water quality, such comprehensive data sets have been less common,
57 but momentum is increasing with QUADICA (Ebeling et al., 2022) and the recently published CAMELS-
58 Chem datasets from the US (Sterle et al., 2024) and from Switzerland (Do Nascimento et al., 2025), which
59 include not only hydroclimatic drivers but also the temporal evolution of pollution sources (e.g.,
60 atmospheric nitrogen deposition and nitrogen surplus as diffuse sources). In parallel, a number of data
61 sets now provide large samples of quality-controlled water quality time series (Zarei et al., 2025; Virro et
62 al., 2021), further complemented by catchment or stream network characteristics (Fernandez et al., 2025;
63 Minaudo et al., 2025).

64 Comprehensive LSH datasets have various applications. They support data-driven top-down approaches
65 to identify trends and patterns in water quantity and quality time series, and when combined with
66 contextual data help advance our understanding of underlying processes and hierarchies. They also
67 provide forcing, calibration, and validation data for hydrological and water quality models (Nguyen et al.,
68 2022; Van Meter and Basu, 2015). The increased availability of LSH datasets also propelled data-driven
69 machine learning (ML) models using them for training, testing, and validation and improving their
70 performance and generalization ability both in time and space (e.g. ungauged basins). ML models are
71 widely applied and improved for discharge predictions (e.g., Kratzert et al., 2018; Heudorfer et al., 2025)

72 but also increasingly used for water quality parameters (Zhi et al., 2023; Zhi et al., 2021; Saha et al.,
73 2023).

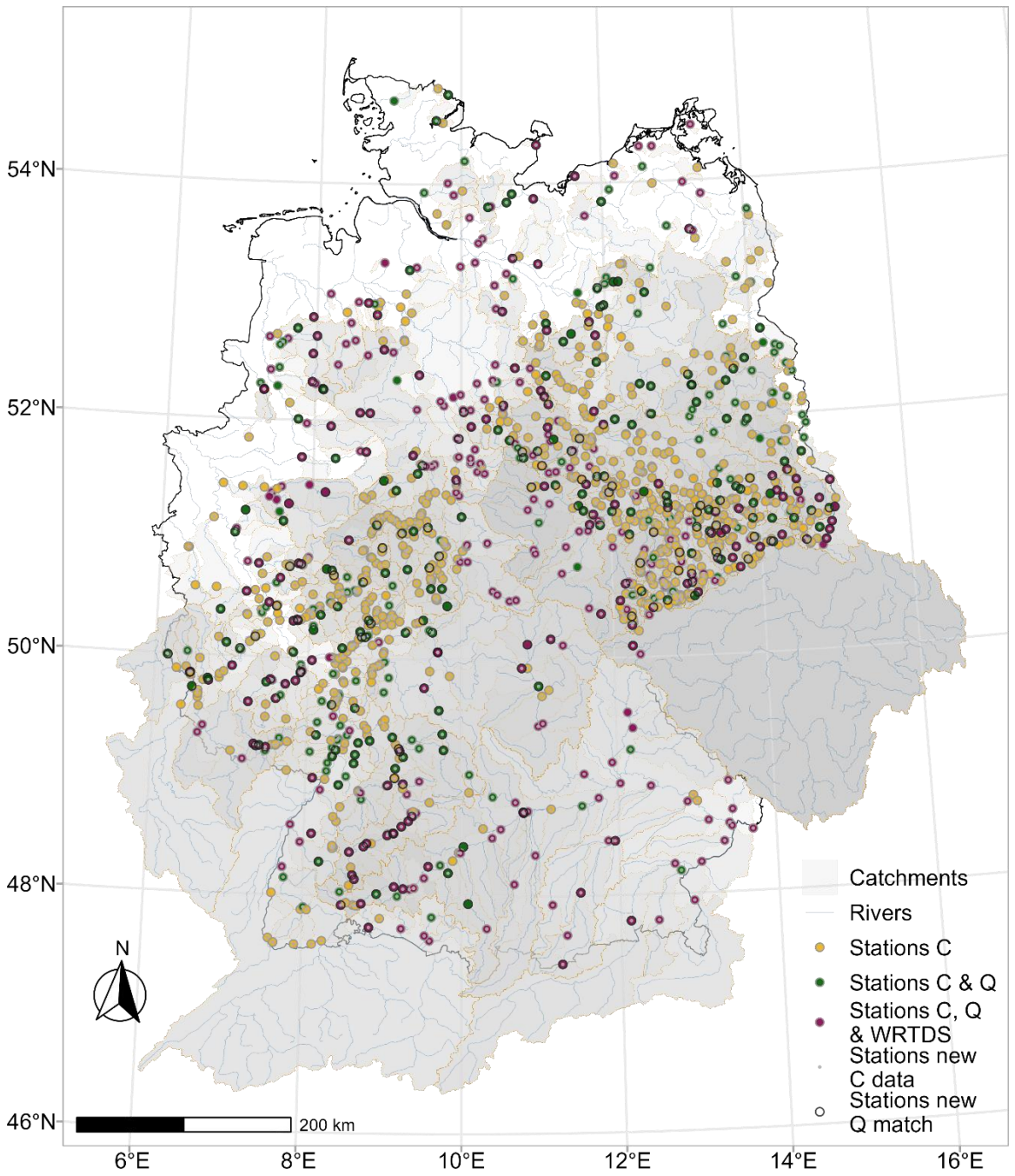
74 Here, we present the second version of QUADICA (water QUAlity, DIcharge and Catchment
75 Attributes), a significant update to the original dataset (Ebeling et al., 2022). The first version of
76 QUADICA has supported a wide variety of water quality studies, including the characterisation of
77 catchments based on nutrient export processes across different spatial and temporal scales (Ebeling et al.,
78 2021b; Ebeling et al., 2021a; Ehrhardt et al., 2021), effects of hydroclimatic extreme events on the
79 catchments' nitrate export (droughts, Saavedra et al., 2024; floods, Saavedra et al., 2022), for nutrient
80 stoichiometric characterisation (Wachholz et al., 2023), as well as for disentangling catchment processes
81 using a process-based water quality model (e.g., Nguyen et al., 2022). A particular focus has been the
82 linkage of observed instream water quality responses to drivers, enabled through the provided catchment
83 attributes and driving forces in the form of diffuse nitrogen sources.

84 Recent shifts in environmental conditions, particularly hydrological extremes such as droughts, have
85 substantial impacts on water quality (Saavedra et al., 2024; Winter et al., 2023; Dupas et al., 2025). This
86 highlights the critical need to extend the QUADICA dataset to include more recent years covering extreme
87 drought years and additional water quality and driver variables, thereby enhancing our ability to
88 understand and address the evolving relationship between environmental change and water quality.
89 Specifically, the update encompasses (1) longer time series up to 2020, capturing recent extreme events
90 such as the 2018-2020 multi-year drought (e.g., Rakovec et al., 2022) with expected effects on solute
91 export (e.g., Winter et al., 2023), (2) additional hydroecological time series such as oxygen and
92 chlorophyll-a concentrations, enabling to move from water quantity and quality to ecological impact
93 studies, (3) additional time series of driving forces including point sources and phosphorus inputs,
94 allowing more comprehensive views on input-output (driver-response) relationships, useful e.g. for the
95 quantification of nutrient legacies or model input data, and (4) larger amount of stations with joint water
96 quantity and quality by linking to the recently published and widely known CAMELS-DE (Loritz et al.,
97 2024) and Caravan-DE (Dolich et al., 2024) data sets. With this updated version, we aim to enhance the
98 breadth of the large-sample water quality dataset QUADICA with additional depth, enabling us to address
99 more research questions and ultimately support water quality management.

100 **2 Station and catchment selection**

101 The 1386 stations and corresponding delineated catchments from the original QUADICA data set
102 (Ebeling et al., 2022) are retained in version 2. Although all stations lie within Germany, 17.9% of the
103 catchments are transboundary with part of their area in a neighbouring country. Figure 1 shows the study
104 area with updated information on the data availability. As for version 1, water quality and quantity data
105 for QUADICA v2 were assembled from the German federal state authorities and merged with the data
106 from QUADICA v1. This allowed us to extend the time series length as well as add new variables of
107 water quality.

108 Similar to version 1, we assessed the data availability after quality control of the water quality time series
109 data. After homogenization of variable names, units and formats across all federal states, the
110 preprocessing steps included: (1) removal of duplicates and implausible values (i.e. zero and negative
111 concentrations), (2) removal of outliers within each time series using a mean plus 4 standard deviations
112 threshold ($> 99.99\% \text{ confidence}$) in logarithmic space for concentrations and normal space for oxygen
113 concentrations (O_2) and water temperature (T), (3) substitution of left-censored values using half of the
114 detection limit, where applicable (i.e. nutrient and mineral concentrations). We additionally removed total
115 organic carbon (TOC) concentrations $> 1000 \text{ mg l}^{-1}$, as we identified implausible plateaus of such high
116 values in three stations, for which the outlier test failed.



117

118

119

120

121

122

123

Figure 1: Stations and delineated catchments in relation to Germany (black line). Stations are colored according to their data availability, with C – concentration (water quality), Q – discharge (water quantity), and WRTDS - Weighted Regression on Time, Discharge and Season. Stations with extended water quality data (new C data) in version 2 are highlighted as well as stations with newly added continuous discharge data (new Q match) from matching with CAMELS-DE (Loritz et al., 2024) and Caravan-DE (Dolich et al., 2024) data sets (for details, refer to Section 3.2). The rivers displayed are taken from (De Jager and Vogt, 2007). WRTDS is available for stations with high data availability (see Section 3.1.2).

124 **3 Time series**

125 Time series data are provided for 1386 catchments (as in QUADICA v1) for water quality variables
126 (Section 3.1) and water quantity (Section 3.2), and forcing variables both from meteorological drivers
127 (Section 3.3) and nutrient (N and P) inputs from diffuse and point sources (Section 3.4). An overview of
128 the provided (and newly added) variables is given in the following and in Table 1, while details are
129 described in the following sections. Appendix B1 provides an overview of data files and respective
130 metadata tables provided in the data repository. Note that due to limited data availability, not all water
131 quality and quantity variables can be provided for all stations.

132 For water quality, QUADICA version 2 increases the number of variables by adding ammonium (NH_4^+ -
133 N) to the previously provided nutrient concentrations (NO_3^- -N, TN, PO_4^{3-} -P, TP, DOC, TOC), major ion
134 concentrations (SO_4^{2-} , Cl^- , Ca^{2+} , Mg^{2+}), concentrations of O_2 and Chlorophyll-a (Chl-a), and water
135 temperature (T). In version 2, dissolved inorganic nitrogen (DIN) was calculated as the sum of the
136 preprocessed time series of inorganic nitrogen forms NO_3^- -N and NH_4^+ -N, and, if available, NO_2^- -N. Note
137 that, for simplicity, the charges are not always written in the following text. For water quantity, the number
138 of stations with discharge data from daily observations was increased from 324 in version 1 to 637 in
139 version 2. For nutrient inputs, time series of catchment-wise diffuse P inputs and point source inputs of
140 N and P were added, while diffuse N sources were both updated as well as extracted from a European
141 data source provided consistently with P.

142

143 **Table 1: Provided time series data, their basis (observed or estimated), aggregation type, temporal resolution and source of original**
144 **data, which was used to calculate the aggregated data provided here. Bold font indicates the newly added variables in version 2 of**
145 **the QUADICA data set. WRTDS -Weighted Regression on Time, Discharge and Season. Note that detailed metadata are provided**
146 **for each data file in the repository, for an overview see Table B1.**

Variable	Section	Data basis	Temporal (Spatial) Aggregation	Temporal resolution	File in repository	Source
Concentrations of nutrient species (NO_3^- -N, NH_4^+-N , DIN, TN, PO_4^{3-} -P,	3.1	observed	median	annual	c_annual.csv	Musolff (2020); Ebeling et al. (2022)
		daily estimated using WRTDS	median	monthly	wrtds_monthly.csv	Musolff (2020); Ebeling et al. (2022)

TP, DOC, TOC, major ions (SO ₄ , Cl, Ca, Mg), O ₂ and Chl-a, and T		observed	long-term median	monthly	c_q_avg_month s.csv	Musolff (2020); Ebeling et al. (2022)
Discharge	3.2	observed	median	annual	q_annual.csv	Musolff (2020); Ebeling et al. (2022); Loritz et al. (2024); Dolich et al. (2024)
		observed	median	monthly	wrtds_monthly.csv	Musolff (2020); Ebeling et al. (2022); Loritz et al. (2024); Dolich et al. (2024)
		observed	long-term median	monthly	c_q_avg_month s.csv	Musolff (2020); Ebeling et al. (2022); Loritz et al. (2024); Dolich et al. (2024)
Precipitation	3.3	observed gridded	sum (average)	monthly	climate_monthly.csv	E-Obs (2018); (Cornes et al., 2018)
Potential evapotranspiration	3.3	estimated	sum (average)	monthly	climate_monthly.csv	E-Obs (2018); (Cornes et al., 2018)
Mean air temperature	3.3	observed gridded	average (average)	monthly	climate_monthly.csv	E-Obs (2018); (Cornes et al., 2018)
Diffuse N (from two sources) and P input as total	3.4	estimated	(average)	annual	input_N_P.csv	see Section 3.4
Diffuse N input from agricultural areas	3.4	estimated	(average)	annual	input_N_P.csv	see Section 3.4
Point source N and P input	3.4	estimated	(average)	annual	input_N_P.csv	see Section 3.4

147

148 **3.1 Water quality time series**

149 After quality control of the time series data, different temporal aggregation schemes were implemented
 150 to provide consistent data sets. In QUADICA version 2, we provide the time series of annual medians

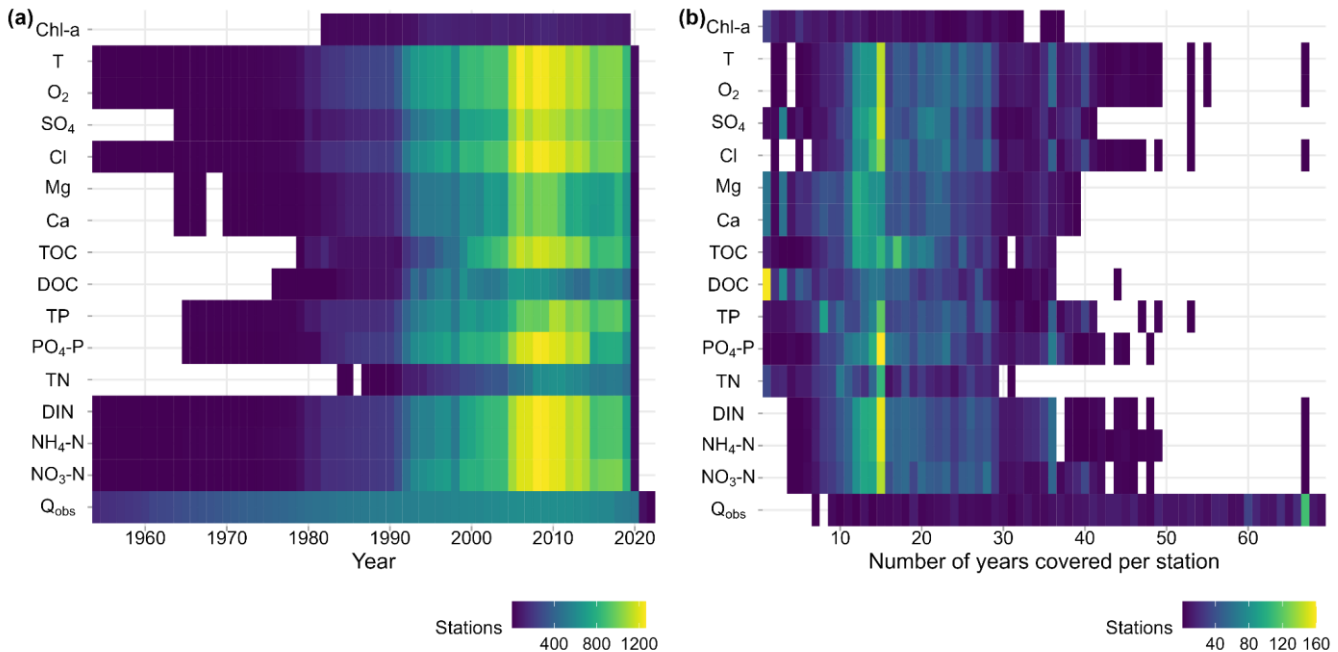
151 (Section 3.1.1), monthly medians for stations with high data availability (Section 3.1.2), and long-term
152 monthly averages (Section 3.1.3).

153 **3.1.1 Annual median water quality variables**

154 Annual median concentrations are provided based on the preprocessed time series (Section 2) for all
155 station-compound combinations. Along with the median concentrations, the number of samples
156 considered for the given value is provided as a control variable for users of the data set, allowing to subset
157 the data based on data availability.

158 The time series of annual median concentrations are visualized in Figures S1 and S2, while the
159 corresponding data density is shown in Figure 2 over the years as well as for the number of years covered
160 per station. A summary of data availability across all variables is provided in Table 2.

161 The highest data availability with more than 1370 stations covered is presented for the inorganic nitrogen
162 ($\text{NO}_3\text{-N}$, $\text{NH}_4\text{-N}$, DIN) and phosphorus ($\text{PO}_4\text{-P}$) compounds, as well as for chloride (Cl), sulfate (SO_4),
163 oxygen (O_2) and water temperature (T). The highest temporal coverage stretches from the mid-2000s to
164 the mid-2010s. Overall, the median time series lengths vary between 13 (for Chl-a) and 24 (O_2 , T) years.
165 The median number of samples per station varies between 104 (for Chl-a) and 205 (for T), while the
166 median average number of samples per year ranges from 10.1 (for DOC) to 11.9 (for $\text{NO}_3\text{-N}$, $\text{PO}_4\text{-P}$, and
167 T) and 12.0 (for Chl-a), i.e. corresponding to a monthly sampling frequency on average.



169

170

171

172

Figure 2: Temporal coverage of water quality and quantity time series data per compound: (a) number of stations with available annual medians per year and compound and (b) the number of years covered by each station per compound. For visualization purposes in (a) station counts from 1950 are shown, omitting one sample before 1954.

173
174
175
176
177
178

Table 2: Summary of stations and data availability for each water quality compound. The table provides the number of stations with the respective compound reported, the earliest and median start year of time series, median and maximum time series length in years across stations as well as the number of covered years (i.e. years with available data, with values provided in parenthesis), total number of grab samples (i.e. data points) for each compound, median number of grab samples per stations and median samples per year and station, number of outliers removed as the sum across all stations, and maximum fraction of outliers removed at one station. n - number, max. - maximum, * omitting one sample from 1900.

Variable	NO ₃ - N	NH ₄ - N	DIN	TN	PO ₄ - P	TP	DOC	TOC	Ca	Mg	Cl	SO ₄	O ₂	T	Chl-a
Unit	mg l ⁻¹	mg l ⁻¹	mg l ⁻¹	mg l ⁻¹	mg l ⁻¹	mg l ⁻¹	mg l ⁻¹	mg l ⁻¹	mg l ⁻¹	mg l ⁻¹	mg l ⁻¹	mg l ⁻¹	mg l ⁻¹	°C	mg l ⁻¹
n stations	1386	1386	1386	782	1379	1301	1167	1323	1337	1337	1380	1375	1379	1379	271
Earliest start year	1954*	1954*	1954*	1984	1965	1965*	1976	1979	1964	1964	1954	1964	1954	1954	1982
Median start year	1995	1997	1997	2005	1995	1996	1995	1999	1997	1997	1994	1997	1993	1993	1996
Median time series length (years covered)	22	20	20	15	21	22	19	20	19	19	23	21	24	24	13
	(18)	(17)	(17)	(14)	(17)	(17)	(13)	(17)	(14)	(15)	(19)	(17)	(20)	(20)	(10)
Max. time series length in years (years covered)	67*	67*	67*	31	53	53*	44	37	49	49	67	53	67	67	37
	(67)	(67)	(67)	(31)	(48)	(53)	(44)	(36)	(39)	(39)	(67)	(53)	(67)	(67)	(37)
Total n samples (excl. outliers)	375,9	364,3	356,2	139,9	350,5	323,5	171,1	291,8	232,9	232,4	372,1	299,4	462,5	396,8	65,63
	90	01	62	48	07	20	23	98	26	12	23	12	08	36	2
Median n samples per station	194	190	190	168	183	177	130	179	145	144	191	181	203	205	104
Median n samples per station and year	11.9	11.8	11.8	11.4	11.9	11.7	10.1	11.7	11.1	11.0	11.8	11.8	11.8	11.9	12
n outliers total	88	292	-	74	212	506	339	950	119	228	666	212	219	8	50
Max. fraction of outliers per station [%]	1.9	3.4	-	2.2	5.8	2.9	3.2	7.2	2.4	3.8	2.3	4.0	2.1	1.1	2.6

179

180 3.1.2 Monthly median concentrations and mean fluxes for stations with high data 181 availability

182 As in version 1 of QUADICA, we provide monthly and annually aggregated water quality data for the 183 subset of stations with high data availability based on Weighted Regression on Time, Discharge and 184 Season (WRTDS; Hirsch et al., 2010), referred to as ‘WRTDS stations’. To fit WRTDS, we used the R 185 package *EGRET* (version 3.0.9; Hirsch and De Cicco, 2015). WRTDS considers long-term trends,

186 seasonal components and discharge-dependent variability to estimate daily concentrations from low-
187 frequency observations, e.g., from monthly grab samples (Hirsch et al., 2010). We included station and
188 compound combinations using the same quality criteria as in QUADICA v1 on the preprocessed
189 concentration data (Section 2). Accordingly, water quality time series had to cover at least 20 years, at
190 least 150 samples, and no data gaps larger than 20 % of the total time series length. Discharge time series
191 with daily temporal resolution are required to run WRTDS, but in contrast to version 1 of QUADICA,
192 gaps in discharge were allowed with the consequence that no concentration estimate is provided for that
193 day. The number of WRTDS stations varies between 97 for TN and 322 for Cl (Table 3), while the fraction
194 of stations with high data availability varies between 12.0 % for TOC and 23.3 % for Cl.
195 As in QUADICA v1, monthly and annual values were only provided if 80% of the days of the respective
196 period were covered. The provided water quality time series contain median concentrations, flow-
197 normalized concentration, and mean flux estimates from WRTDS models. We now also added discharge-
198 weighted mean concentrations. Discharge corresponds to the median observed, as WRTDS takes
199 discharge as input and does not modify it (Section 3.2.2).
200 The model performance of WRTDS varies across water quality variables and stations with 64.1% of the
201 station and compound combinations with $R^2 > 0.5$ and 58.2% with a percent bias $< 1\%$ and 92.7% below
202 $< 5\%$. Average performances per compound are given in Table 3, while the distribution of performance
203 values is provided in Figure A3, as well as all individual values provided in the repository. The
204 performance metrics should allow the users to select suitable catchments and compounds for reliable
205 analysis.
206

207

208

209

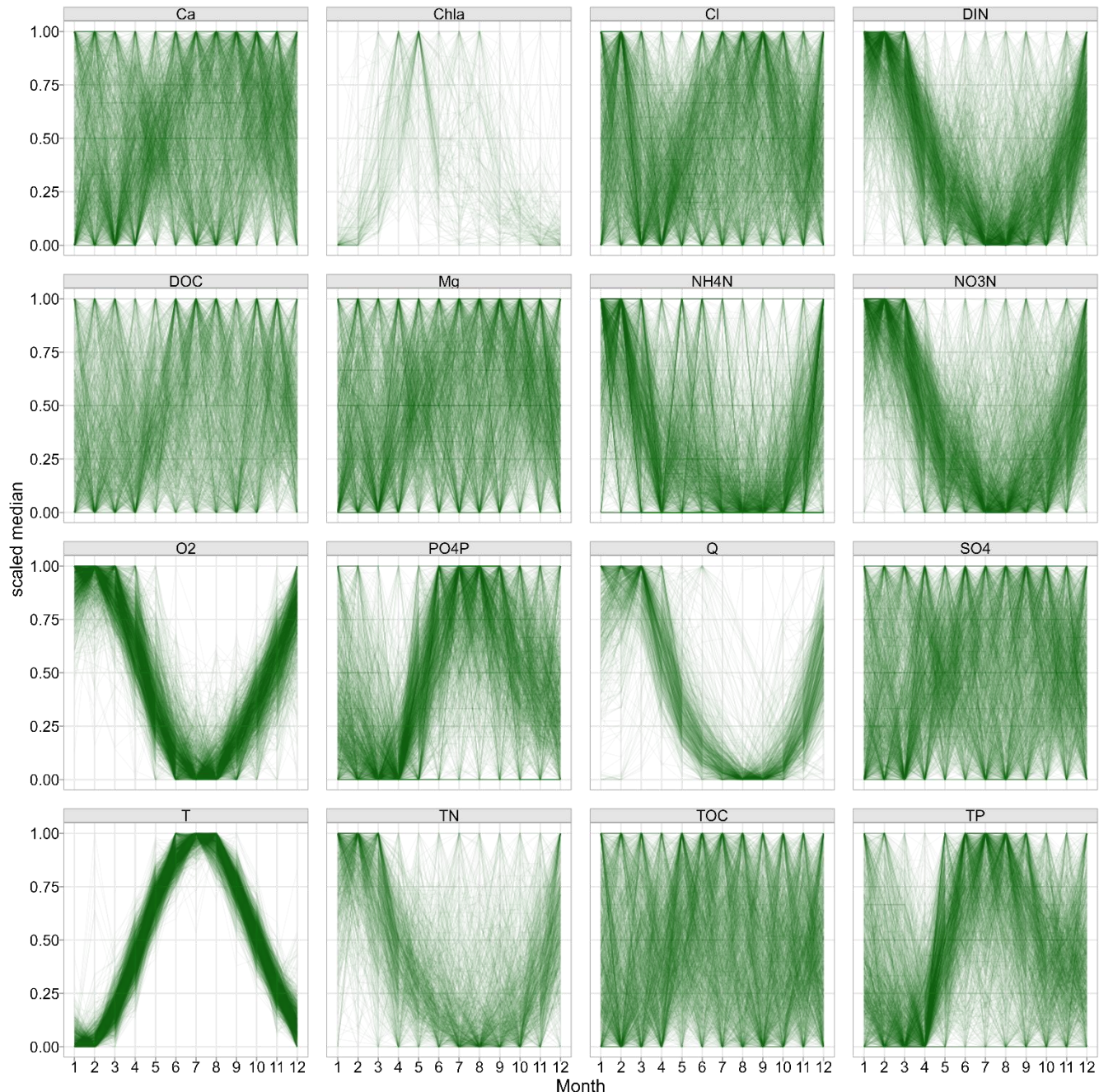
Table 3: Number of stations with high data availability (WRTDS stations) for each compound and median coefficient of determination of WRTDS models. The unit of all variables is mg l⁻¹.

Variable	Number of WRTDS stations	Median R ²	Median bias [%]
total	347	0.58	-4.9*10 ⁻²
NO₃-N	317	0.64	0.20
NH₄-N	302	0.48	0.96
DIN	303	0.68	0.18
TN	97	0.71	5.1*10 ⁻³
PO₄-P	288	0.62	-0.73
TP	270	0.48	-0.53
DOC	140	0.45	-0.65
TOC	195	0.46	-0.40
Ca²⁺	175	0.62	2.8*10 ⁻²
Mg²⁺	174	0.57	-6.6*10 ⁻²
Cl	322	0.53	-3.9*10 ⁻²
SO₄	234	0.67	5.5*10 ⁻²

210

211 3.1.3 Monthly long-term median concentrations

212 To be consistent with QUADICA v1, we provide monthly long-term medians, and 25th and 75th
 213 percentiles (i.e. interquartile range), providing information on the average seasonality patterns of each
 214 respective time series. Figure 3 shows the scaled medians indicating the variability of seasonal timing
 215 across stations for each compound. For example, water temperature and oxygen show very similar
 216 seasonality in terms of timing with summer maxima and summer minima, respectively, in contrast to,
 217 e.g., Ca²⁺, Mg²⁺, DOC and TOC, for which seasonal timing varies strongly across stations. The nitrogen
 218 and phosphorus species show dominant seasonal patterns, but still more variability across stations.



219

220
221

Figure 3: Median monthly water quality observations inform about seasonal variability. Medians at each station are scaled to a range between 0 and 1. Note that only time series covering all 12 months are displayed.

222 **3.2 Water quantity time series**

223 In total, discharge was provided for 637 stations, taking all data sources together. The earliest time series
224 starts in 1893, the maximum number of stations with 620 stations with available discharge data was in
225 2011 and the longest time series extends until 2022.

226 From the QUADICA v1, we updated the discharge time series of 284 out of the 324 stations with daily
227 data provided from our request to the authorities (232) and from GRDC (52) based on the matches
228 identified in QUADICA v1. For the remaining stations, no updated data was provided.

229 In addition, we complemented the QUADICA discharge data from the CAMELS-DE (Loritz et al., 2024)
230 and Caravan-DE (Dolich et al., 2024) data sets. We found 554 matches (449 from CAMELS, 105 from
231 Caravan), out of which 313 stations had no matching discharge values in QUADICA yet, while 241
232 overlapped. We matched stations based on location and by manually checking if they lie on the same
233 river. We differentiate cases between (1) close stations within a maximum distance of 1km (n=305) and
234 (2) discharge stations that are further away. In the latter case, discharge stations could be located either
235 (2i) upstream (n=202) or (2ii) downstream (n=47) of the water quality station. For (2), we accepted
236 matches only if the relative difference between the intersected area of the CAMELS/Caravan and
237 QUADICA catchments and the area of the QUADICA catchment was $\leq 30\%$. For downstream discharge
238 stations (2ii), in addition, we accepted matches only if the CAMELS area was larger than the QUADICA
239 area.

240 We additionally checked the correlations between QUADICA and CAMELS/Caravan time series with a
241 median correlation coefficient of $r>0.9999$ and only 5 out of the 241 overlapping stations with $r<0.95$.
242 We then used the discharge time series of the matched stations to fill up the QUADICA data. To account
243 for differences in the locations (and thus catchments' area) of water quantity and water quality stations,
244 we scaled the discharge of upstream discharge stations (i.e. case 2i) with the ratio between the QUADICA
245 catchment area to the intersected area and of downstream stations (i.e. case 2ii) with the ratio between the
246 QUADICA to CAMELS/Caravan catchment area. In case of several potential matches (because of
247 identical station locations within CAMELS, n=24), we manually checked the time series to decide for the
248 more complete one or merged them with priority on the more recent time series (n=2).

249 **3.2.1 Annual median discharge**

250 Similar to version 1, annual median discharge is aggregated from available observed discharge data. As
251 described above (Section 3.2), daily Q data is available for 637 water quality stations. The data density
252 distribution is visualised in Figure 2.

253 **3.2.2 Monthly median discharge**

254 Similar to version 1, monthly median discharge is provided for WRTDS stations. Note that we did not
255 gap-fill the daily discharge time series for the WRTDS models, but instead provide median values only
256 if at least 80% of the days are covered. This criterion refers both to the monthly and annual discharge data
257 provided with the WRTDS data tables (as described in Section 3.1.2).

258 **3.2.3 Monthly long-term median discharge**

259 Similar to version 1 of QUADICA and the water quality variables (Section 3.1.3), long-term monthly
260 median discharge, 25th and 75th percentiles, as well as the corresponding number of samples are provided.
261 These values can be an indicator of average discharge seasonality across solutes and catchments in the
262 long term.

263 **3.3 Meteorological time series**

264 As in QUADICA v1, meteorological time series (precipitation, potential evapotranspiration and average
265 air temperature) are provided as spatial catchment averages on monthly resolution from 1950 to 2020. To
266 obtain these, we followed the same approach on a newer version from the European Climate Assessment
267 and Dataset project (E-Obs, 2018; Cornes et al., 2018) for the daily gridded data of climate variables.
268 Moreover, for the stations for which we identified matches from the CAMELS-DE/Caravan-DE datasets
269 the users can access daily time series of several hydrometeorological variables and different products
270 therein (Dolich et al., 2024; Loritz et al., 2024). However, note that the water quality stations are not
271 always located at the exact same location, please refer to Section 3.2 and the details provided in the data
272 repository and data tables about the matches.

273 **3.4 N and P input time series**

274 **3.4.1 Net N and P input from diffuse sources**

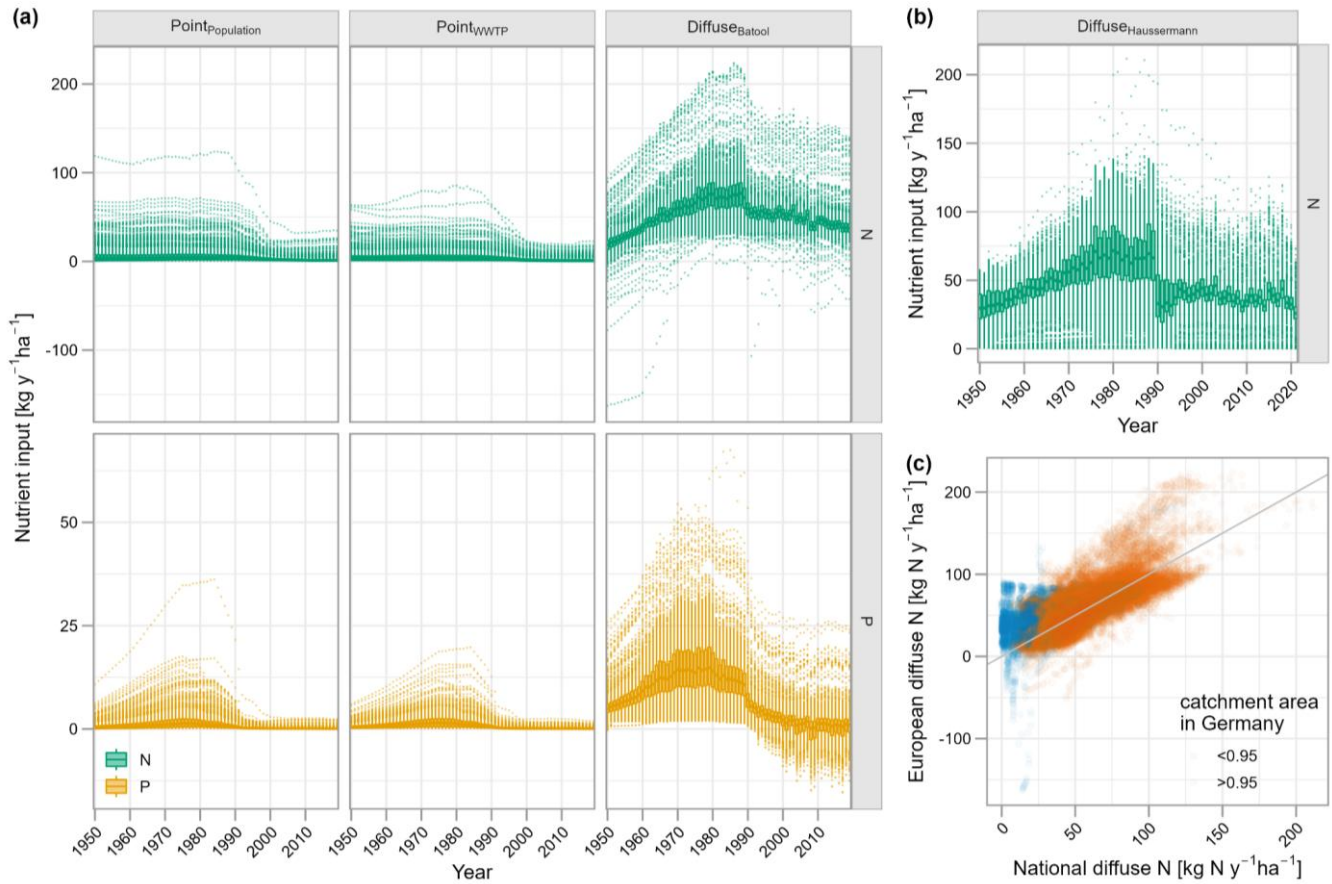
275 Time series of catchment-scale N and P surplus ($\text{kg y}^{-1} \text{ ha}^{-1}$) from diffuse sources as shown in Figure 4
276 are provided (file: input_N_P.csv). The catchment-scale surplus corresponds to a soil surface budget and
277 equals the balance between nutrient inputs minus the output on agricultural and non-agricultural areas at
278 an annual resolution normalized to the catchment area. Inputs include mineral fertilizer, manure, other
279 organic fertilizers (in the German N surplus dataset only; such as sewage sludge, compost and biogas
280 digestate), atmospheric deposition, biological fixation (N surplus only), weathering (P surplus only) and
281 seeds and planting material (in the German N surplus dataset only). Outputs correspond to crop and
282 pasture removal.

283 For N surplus, two different data sets were used: 1. A Germany-wide county-scale data set as described
284 in depth in QUADICA v1 (Ebeling et al., 2022; Behrendt et al., 2003; Häußermann et al., 2020), and 2.
285 A European gridded data set (Batool et al., 2022).

286 For the first source of N surplus, the N surplus time series on agricultural areas were updated with the
287 German data provided by Häußermann et al. (2020) for the period 1995-2021, following Ebeling et al.
288 (2022). However, we refined the methodology to account for temporarily variant agricultural areas,
289 following Sarrazin et al. (2022). The data now ranges from 1950-2021 (1950-2015 in the previous
290 version). We extended the N surplus from non-agricultural areas until 2021 by calculating the sum of
291 atmospheric deposition and biological N fixation as described in QUADICA v1. Note that the values for
292 transnational catchments have higher uncertainties as they were calculated for the area within Germany
293 only (for the corresponding fraction, see f_areaGer).

294 For the second source of N surplus, N surplus time series were extracted from a gridded, European-scale
295 dataset (Batool et al., 2022) providing annual estimates of N surplus from 1850 to 2019 at 5 arcmin (~10
296 km at the equator) resolution. It covers both agricultural and non-agricultural soils. The N surplus time
297 series across catchments from both sources are compared in Figure 4c, while a comparison of the datasets
298 can be found in Batool et al. (2022). Overall, there is a correlation with $r=0.72$ across all catchments,
299 which increases to $r=0.76$ when considering only the catchments with at least 70%, 95% or a 100% of

300 their catchment area within Germany. Additionally, differences can arise from methodological and scale
 301 differences as well as uncertainties in general.



302
 303 **Figure 4:** Nitrogen and phosphorus input time series from different sources shown as distributions across all catchments. In (a) point
 304 sources data comes from Sarrazin et al. (2024) Sarrazin et al. (2024) corresponds to the ensemble mean from two different spatial
 305 disaggregation approaches based on population density (Point_{Population}) and WWTP data (Point_{WWTP}) (Section 3.4.2) and the
 306 ensemble mean of diffuse sources input of N from Batool et al. (2022) and of P from Batool et al. (2025) (Diffuse_{Batool}). In (b) diffuse
 307 source of N from Häußermann et al. (2020) is shown, while in (c) the diffuse N input values for each year and each catchment of the
 308 two data sets (from the German and European data basis) are compared, with the color indicating the fraction of catchment area
 309 within German boundaries (orange - ≥ 0.95 , blue - < 0.95). Note that: The boxes of the boxplots show the median, the 25th and 75th
 310 percentiles, while the whiskers extend up to 1.5*interquartile ranges with outliers beyond this range; Y axis scale is different for N
 311 and P.

312 For P surplus, we used the European-scale dataset (Batool et al., 2025) constructed with the same spatial
 313 and temporal resolution and a similar methodology as the one of N surplus. Both European datasets
 314 quantify uncertainties in key components such as fertilizer use, manure allocation, and crop removal. For
 315 QUADICA, we extracted the ensemble mean of the total N and P surplus estimates to assess diffuse

316 nutrient inputs relevant at the catchment scale. For further details on the data uncertainty, please refer to
317 (Batool et al., 2022; Batool et al., 2025).

318 **3.4.2 N and P input from point sources from wastewater**

319 While in QUADICA v1, point source data are available for only one year (around 2016), QUADICA v2
320 provides time series of N and P point source inputs from wastewater for each catchment for the period
321 1950-2019. The data come from the gridded dataset of Sarrazin et al. (2024) for Germany. This data set
322 provides estimates of N and P point sources, accounting for wastewater emissions that are treated in urban
323 Wastewater Treatment Plants (WWTPs), including domestic and industrial (indirect) emissions, as well
324 as untreated domestic emissions collected in the sewer system. These treated and untreated N and P
325 emissions result from human excreta, with additional emissions for P due to the use of detergents. The
326 data were constructed combining a modelling approach and observational data of WWTP N and P
327 emissions. Sarrazin et al. (2024) provides ensemble runs from two methods to spatially disaggregate the
328 data to grid resolution, that is, one based on population density and the other one based on recent WWTP
329 outgoing N and P emissions. QUADICA v2 includes, for each catchment, two point source time series
330 corresponding to the respective ensemble means of the two disaggregation approaches. For further details
331 including time-dependent uncertainty of the two methods due to the shift in information detail and
332 corresponding representativeness, please refer to Sarrazin et al. (2024).

333 **4 Catchment attributes**

334 The catchment attributes describe the topography, land cover, nutrient sources, lithology, and soils, and
335 hydroclimate of the catchments. The attributes provided in QUADICA v1 were partly updated and
336 complemented. New attributes include the Strahler order, updated land cover fractions from the CORINE
337 Land cover dataset for 2018, the mean monthly Leaf Area Index (LAI), the soil pH in water and in CaCl_2 -
338 solution as well as updated average nutrient source and hydroclimatic characteristics. Here, we describe
339 only updated and complemented characteristics; for a detailed description of the previous characteristics,
340 please refer to QUADICA v1 (Ebeling et al., 2022). The metadata table of all characteristics in QUADICA

341 v2 is provided in Appendix B2 and Table S11 in the metadata of the data repository, while the attributes
342 data can be found in the file attributes.csv (see Appendix B1).

343 **4.1 River network position**

344 In the version 2 of QUADICA, we add the attribute of stream Strahler order, derived from the EU Hydro
345 data set (EEA, 2020). For each catchment, the largest Strahler order of streams intersecting the catchment
346 was selected and manually checked. The Strahler order provides context of the size and position of the
347 streams with headwater streams starting with Strahler order 1, going up to the order 8 for the downstream
348 part of the Elbe river. Most streams classify as order 3 (n=417) and 2 (n=321), i.e. small to medium sized
349 rivers.

350 To further support network analyses, we link each station to its next downstream station in the river
351 network and count the number of upstream stations, enabling spatially consistent analyses and modelling
352 of water quality patterns and network connectivity. More than half of the stations (731) have no station
353 further upstream, while 95 have no further downstream station.

354 **4.2 Land cover**

355 The fractions of land cover classes were calculated from the CORINE Land cover map (as in QUADICA
356 v1) but with the newer data set for 2018 (version 2020_20u1; EEA, 2019). We both provide level 1
357 (artificial, agricultural, forested land, wetland, and surface water cover) as well as level 2 data with refined
358 classes, as described in APPENDIX B.

359 For each catchment, the mean monthly LAI across the period 2003-2020 was extracted from high-quality
360 reprocessed MODIS LAI data (Yan et al., 2024). Generally, the LAI is defined as the ratio of green leaf
361 area to unit ground surface area, which can be estimated from spectral remote sensing data. The LAI
362 serves as an indicator for e.g. photosynthesis, evapotranspiration and rainfall interception capabilities of
363 vegetated areas.

364 **4.3 Nutrient sources**

365 Average inputs of nitrogen and phosphorus from diffuse and point sources for each catchment are
366 provided based on the respective annual time series described in Section 3.4. We calculated the mean
367 values starting from 1991 (i.e. 1991-2021 in case of Häußermann and 1991-2019 in case of Batool and
368 Sarrazin), representing long-term average historic inputs since the year the Nitrate Directive was amended
369 (EC, 1991). In addition, we calculated mean values over the last decade starting in 2010, representing
370 current nutrient pollution pressures. We also renewed the measure of N source apportionment considering
371 the data sets covering the same spatial scale for Germany, i.e. using the updated data product of the
372 German-wide N surplus data and the newly added N point source data set for both the long-term period
373 and the recent decade.

374 In addition, we provide catchment-averages of soil P budget data from the European data set provided by
375 Panagos et al. (2022). The data set provides maps for P available for crops and P total in agricultural
376 topsoil (0-20 cm) based on the Land Use and Cover Area frame Survey (LUCAS) as raster data with
377 500m resolution, as well as the soil P input and output budget components over the period 2011-2019.
378 The input components inorganic fertilizers and manure are provided as vector data at NUTS
379 (Nomenclature of Territorial Units for Statistics) 2 level, whereas the atmospheric deposition and
380 chemical weathering data are in raster format. The extracted output components include the output
381 through crop harvesting and removal of crop residues, both provided at NUTS2 level. Based on that we
382 calculated the P surplus as a balance component at the soil level. For raster data we calculated the mean
383 across each catchment, providing available and total P on agricultural soils, and scaled it to the catchment
384 area by the fraction of agriculture based on CORINE land cover data (EEA, 2016). To estimate the
385 catchment-scale values from the data sets at NUTS2 level, we first intersected them with the catchments,
386 second calculated the fraction of agriculture to scale the input and output components, and finally
387 calculated area-weighted means for each catchment.

388 **4.4 Soil properties**

389 In addition to average total soil nutrient content in the topsoil (0-20 cm), we added data on average soil
390 pH. The topsoil pH in water and CaCl_2 0.01 M solution was derived from the European soil chemistry

391 map, which is based on the LUCAS database (Ballabio et al., 2019). Historically, soil pH was often only
392 measured in water. However, soil pH measured in a salt solution of CaCl_2 or KCl is now preferred, as it
393 is less affected by electrolyte concentrations in the soil and thus provides a more consistent measurement
394 of fluctuating salt content (Minasny et al., 2011). For comparability, the mean topsoil pH from both
395 methods was extracted for each catchment.

396 **4.5 Hydroclimatic characteristics**

397 The hydrologic characteristics such as mean discharge and metrics of discharge variability were
398 calculated from the updated observed daily discharge data for 637 stations (Section 3.2). We calculated
399 long-term time series characteristics starting in November 1990 (hydrological year of 1991) until October
400 2020, i.e. covering 30 years if available. The exact starting and ending dates used for calculation are
401 provided along with the characteristics, as well as information on missing values. For a list of
402 characteristics, refer to Appendix B and the data repository. For those stations matching with CAMELS-
403 DE/Caravan-DE (Dolich et al., 2024; Loritz et al., 2024), further hydrometeorological characteristics can
404 be accessed directly from these datasets.

405 **5 Limitations**

406 Although some of the previously discussed limitations have been addressed, other limitations and
407 uncertainties remain present in QUADICA v2.

408 We significantly increased the number of stations with discharge from daily time series and thus the
409 number of stations with high data availability (WRTDS-stations) more than doubled to now 347 in total.
410 Still, co-located water quantity and quality stations remain limited with less than half of the stations
411 covered (637 out of 1386 stations).

412 Unfortunately, one of the main drawbacks related to data policies remains. More specifically, data handed
413 over by federal state agencies cannot generally be handed over to third parties, so raw data of water quality
414 and quantity cannot be provided here. We thus adhere to the provision of ready-to-use aggregated data,
415 which can still serve various purposes, e.g. trend analysis (Ehrhardt et al., 2021) and long-term water
416 quality modelling (Nguyen et al., 2022).

417 Uncertainties related to transboundary catchments (beyond the German borders) were reduced for the
418 diffuse nutrient input time series by integrating the European data sets that have become available.
419 However, the uncertainty for the point source time series, which only includes German territory, remains
420 high and such stations may be excluded for certain analysis. For the diffuse N inputs, both time series
421 from German as well as European data bases are provided enabling direct comparison to assess reliability
422 and uncertainty related to the input time series.

423 **6 Data availability**

424 The data set can be accessed in the data repository under
425 <https://doi.org/10.4211/hs.c2866cd416b94ca386deb5758834311f> (Ebeling et al., 2025). It includes all
426 time series, catchment attributes and summary data as well as detailed data description files. Alongside
427 with the repository, we provide an interactive R Shiny application that allows users to check data coverage
428 and visualise selected time series. In addition, a browser-based web app is available for exploring the data
429 set through the institutional UFZ GeoData Infrastructure, accessible at <https://web.app.ufz.de/gdi/wq-monitor/en>. Due to license agreements, the raw data itself cannot be published but are deposited in a long-
430 term institutional repository (Musolff et al., 2020), for which metadata are deposited in a freely accessible
431 repository (Musolff, 2020).

433 **7 Conclusions**

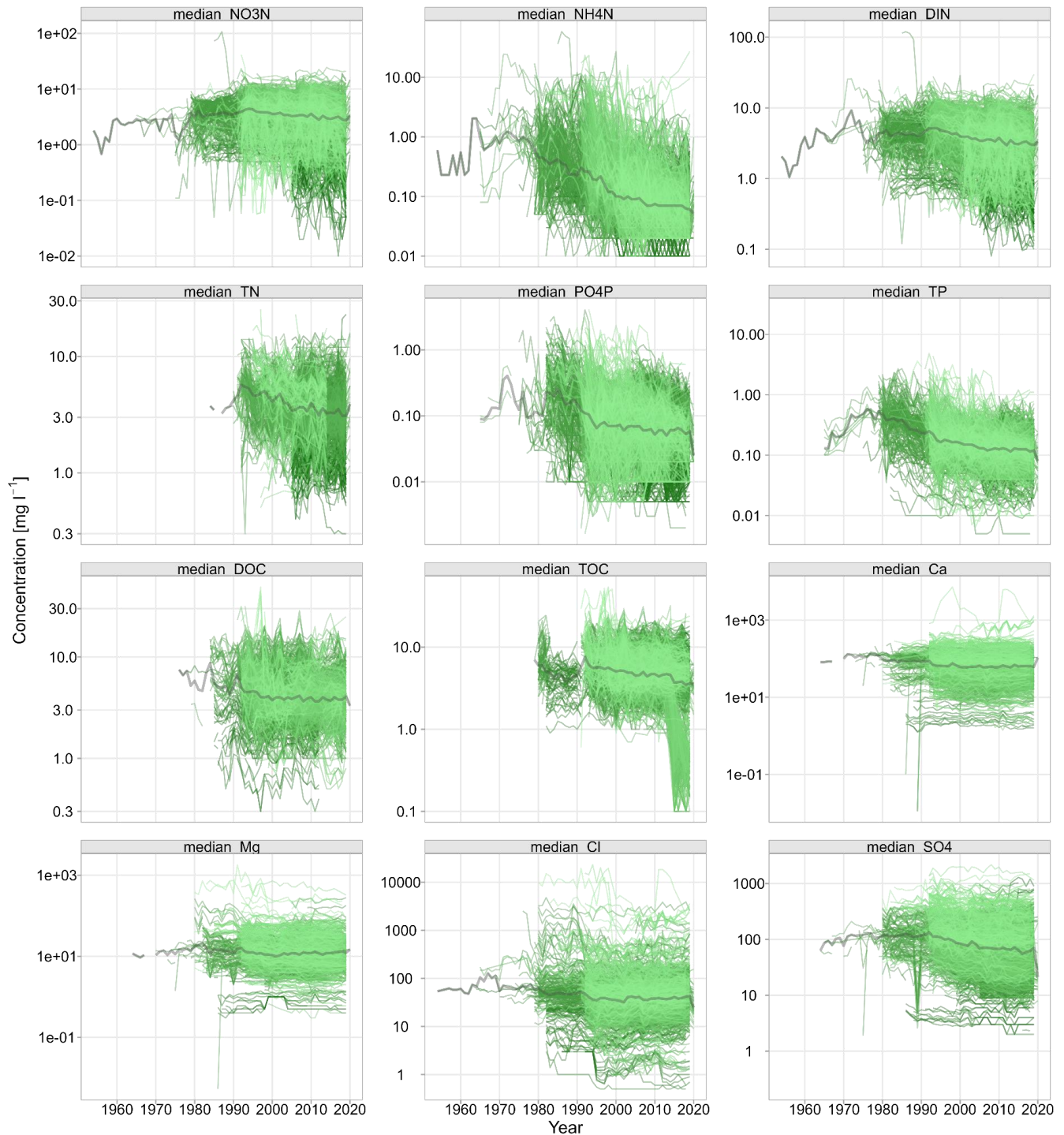
434 This paper aims to provide an updated and extended version of the QUADICA data set for Germany
435 (Ebeling et al., 2022) to enhance both the breadth and the depth (Gupta et al., 2014). Therefore, we focused
436 on describing the new additions in more detail. The main novelties are:

- 437 • Extension of water quality and quantity time series for four years up to 2020, covering severe
438 drought years and generally longer time series (Section 3.1 and 3.2)
- 439 • New water quality parameters were added including those relevant for ecological impact studies
440 such as oxygen, water temperature and chlorophyll-a concentrations (Section 3.1)

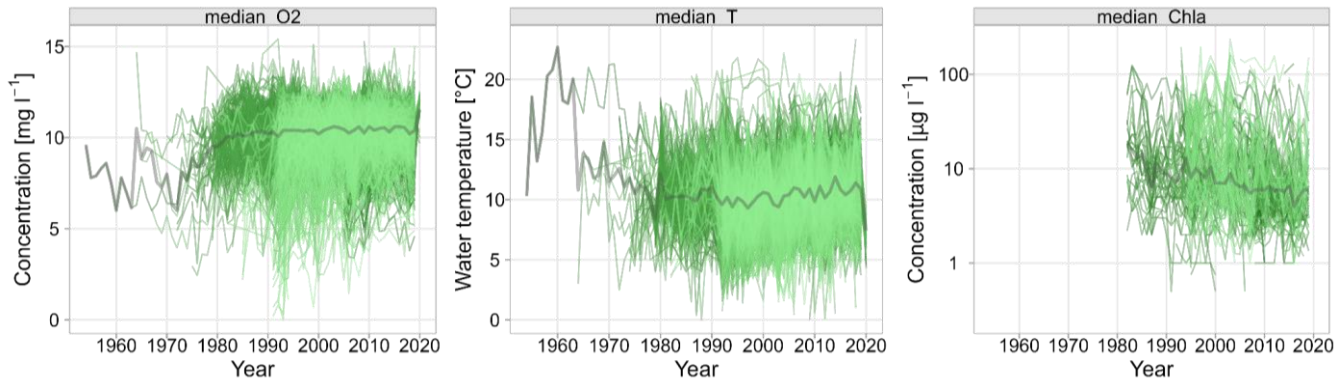
- Linkage to recently published large-sample water quantity data sets for Germany (CAMELS-DE by Loritz et al. (2024) and Caravan-DE by Dolich et al. (2024)) almost doubled the number of water quality stations with conjunctive continuous discharge data from 324 (version 1) to 637 (version 2), allowing for more comprehensive studies of water quantity and quality (Section 3.2)
- The increase in stations with daily discharge data has also increased the number of stations with high data availability (version 2: 347, before: 140) with monthly concentration time series derived from WRTDS models (Section 3.1.2)
- Addition of diffuse phosphorus input and nitrogen and phosphorus point source input time series for German catchments (Section 3.4)
- Addition and update of catchment characteristics including network position (Section 4)

These additions allow for further comprehensive investigations from drivers of nutrient pollution to water quality responses in streams, including ecological implications, and conjunctive water quality and quantity assessment.

454 **Appendix A**



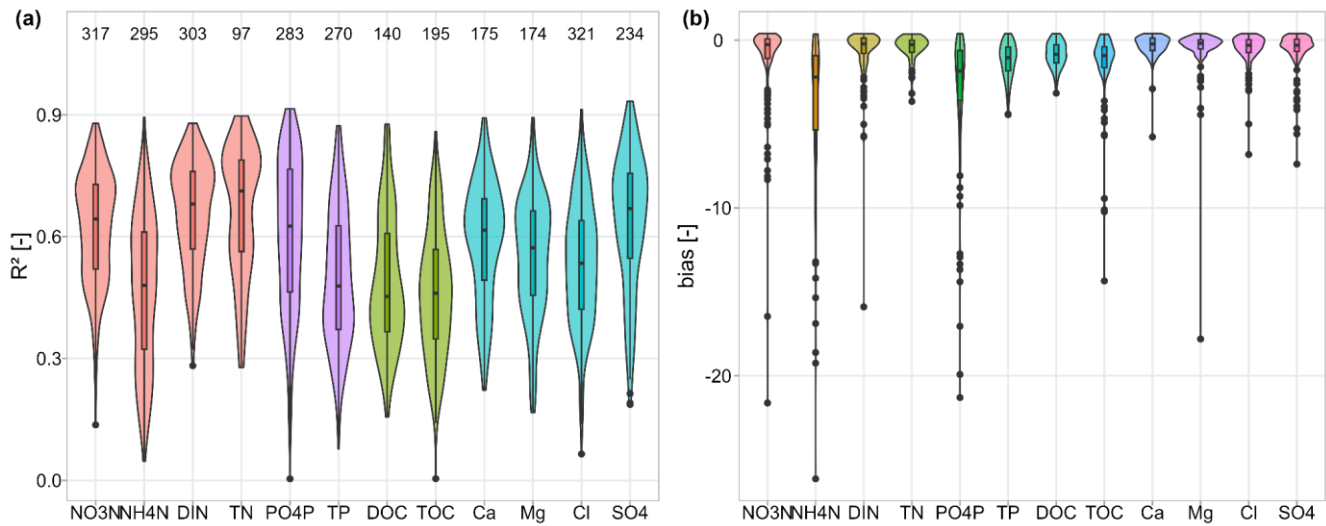
455
 456 **Fig. A1: Annual median concentrations observed at the 1386 water quality stations (described in Table 1, Fig. 1 and Section 3.1).**
 457 The colors are gradual from light to dark corresponding to the OBJECTID numbers, the grey line shows the median concentration
 458 across all annual medians.



459

460 **Fig. A2:** Annual median O₂ concentrations, water temperature, and chlorophyll-a concentration observed at the 1386 water quality
 461 stations (described in Table 1, Fig. 1 and described in Section 3.1). The colors are gradual from light to dark corresponding to the
 462 OBJECTID numbers.

463



464

465 **Fig. A3:** WRTDS-model performances for each compound: (a) coefficient of determination R² and (b) bias. Boxes highlight the
 466 median and quartiles of each distribution. In (a) the number of time series is given on top for each compound. Colors according to
 467 the substance group, i.e. nitrogen, phosphorus, organic carbon and major ions. Note that in (a) values of R²<0 were omitted,
 468 accounting seven catchments for NH₄-N, five for PO₄-P, and one for Cl; in (b) values of bias < -30 were omitted, accounting five
 469 values of NH₄-N and one value for Cl. The users can define their quality criteria to subset the provided time series.

470

471 **Appendix B**

472 **Table B1: Overview of files and metadata tables in the description file (Metadata_QUADICA_v2.pdf) of the data repository.**

Table in metadata file	Data file in repository	Corresponding section in manuscript
S1	metadata_c.csv	3.1 general
S2	metadata_q.csv	3.2 general
S3	wrtds_summary.csv	3.1.2, 3.2.2
S4	c_annual.csv	3.1.1
S5	c_q_avg_months.csv	3.1.3, 3.2.3
S6	wrtds_monthly.csv, wrtds_annual.csv	3.1.2, 3.2.2
S7	q_annual.csv	3.2.1
S8	climate_monthly.csv	3.3
S9	input_N_P.csv	3.4
S10 (same as Table B2)	attributes.csv	4

473

474 **Table B2: Catchment attributes, associated methods and original data sources used for calculating the attributes. It contains both**
475 **attributes from QUADICA v1 and the newly added and updated attributes. For more details see Section 4, data file: attributes.csv.**

Category	Variable	Unit	Description and method	Data source
General	OBJECTID	-	Unique identifier	
	Station	-	Station name	
	Area_km2	km ²	Catchment area	
	f_AreaGer	-	Fraction of catchment area within Germany	
Network	strahler_order	-	Strahler order based on EU Hydro river network	EEA (2020)
	id_downstream	-	OBJECTID of next downstream station	
	n_upstream	-	Number of upstream stations	
Topography	dem.mean	mamsl	Mean elevation of catchment, from DEM rescaled from 25 to 100 m resolution using average	EEA (2013)
	dem.median	mamsl	Median elevation of catchment, from DEM rescaled from 25 to 100 m resolution using average	EEA (2013)

slo.mean	°	Mean topographic slope of catchment, from DEM	EEA (2013)
slo.median	°	Median topographic slope of catchment, from DEM	EEA (2013)
twi.mean	-	Mean topographic wetness index (TWI, Beven & Kirkby, 1979)	EEA (2013)
twi.med	-	Median topographic wetness index (TWI, Beven & Kirkby, 1979)	EEA (2013)
twi.90p	-	90 th percentile of the TWI as a proxy for riparian wetlands (following Musolff et al., 2018)	EEA (2013)
ddhad	km ⁻¹	Average drainage density of the catchment. Gridded drainage density is provided as the length of surface waters (rivers and lakes) per area from a 75km ² circular area around each cell centered.	BMU (2000)
DrainDens	km ⁻¹	Average drainage density of the catchment, calculated from EU-Hydro River Network and intersection with Catchment polygons (contains several implausible values (often too small values due to coarser resolution of river network))	EEA (2016b)
Land cover			
f_artif,	-	Fraction of artificial land cover based on CORINE map from 2012 (f_artif) and 2018 (f_artif_18)	EEA (2016a), EEA (2019)
f_artif_18			
f_agric,	-	Fraction of agricultural land cover based on CORINE map from 2012 (f_agric) and 2018 (f_agric_18)	EEA (2016a), EEA (2019)
f_agric_18			
f_forest,	-	Fraction of forested land cover based on CORINE map from 2012 (f_forest) and 2018 (f_forest_18)	EEA (2016a), EEA (2019)
f_forest_18			
f_wetl,	-	Fraction of wetland cover based on CORINE map from 2012 (f_wetl) and 2018 (f_wetl_18)	EEA (2016a), EEA (2019)
f_wetl_18			
f_water,	-	Fraction of surface water cover based on CORINE map from 2012 (f_water) and 2018 (f_water_18)	EEA (2016a), EEA (2019)
f_water_18			
f_urban,	-	Fraction of Class 11 Level 2 CORINE Land Cover	EEA (2016a), EEA (2019)
f_urban_18			

f_industry,	-	Fraction of Class 12 Level 2 CORINE Land Cover	EEA (2016a), EEA (2019)	
f_mine,	-	Fraction of Class 13 Level 2 CORINE Land Cover	EEA (2016a), EEA (2019)	
f_urban_veg,	-	Fraction of Class 14 Level 2 CORINE Land Cover	EEA (2016a), EEA (2019)	
f_urban_veg_18	-	Fraction of Class 21 Level 2 CORINE Land Cover	EEA (2016a), EEA (2019)	
f_agri_perm,	-	Fraction of Class 22 Level 2 CORINE Land Cover	EEA (2016a), EEA (2019)	
f_agri_perm_18	-	Fraction of Class 23 Level 2 CORINE Land Cover	EEA (2016a), EEA (2019)	
f_agri_hetero,	-	Fraction of Class 24 Level 2 CORINE Land Cover	EEA (2016a), EEA (2019)	
f_agri_hetero_18	-	Fraction of Class 31 Level 2 CORINE Land Cover	EEA (2016a), EEA (2019)	
f_forest,	-	Fraction of Class 32 Level 2 CORINE Land Cover	EEA (2016a), EEA (2019)	
f_forest_18	-	Fraction of Class 33 Level 2 CORINE Land Cover	EEA (2016a), EEA (2019)	
lai_01,	lai_12	Monthly mean leaf area index (LAI) as catchment average. The number indicates the month from 1 for January to 12 for December.	Yan et al. (2024)	
pdens	inhabitants km ⁻²	Mean population density	CIESIN (2017)	
Nutrient sources	Nsurp_Haussermann_from1991, Nsurp_Haussermann_from2010	kg N ha ⁻¹ y ⁻¹	Mean nitrogen (N) surplus per catchment from the German wide data set based on Häußermann et al. (2020) during the period 1991-2021 (from1991) and 2010-2021 (from2010). It includes the N surplus on agricultural and non-agricultural areas. Details in Section 3.4.	Bach et al. (2006); Bach and Frede (1998); Bartnicki and Benedictow (2017); Bartnicki and Fagerli (2006); Behrendt et al. (1999); Cleveland et al. (1999); Häußermann et al. (2020); Van Meter et al. (2017)
Nsurp_Batool_from1991, Nsurp_Batool_from2010	kg N ha ⁻¹ y ⁻¹	Mean nitrogen (N) surplus per catchment from the European data set (Batool et al., 2022) during the period 1991-2021 (from1991) and 2010-2021 (from2010). It includes the N surplus on agricultural and non-agricultural areas. Details in Section 3.4.	Batool et al. 2022	

Psurp_Batool_f rom1991, Psurp_Batool_f rom2010	kg N ha ⁻¹ y ⁻¹	Mean phosphorus (P) surplus per catchment from the European data set (Batool et al., 2024) during the period 1991-2021 (from1991) and 2010-2021 (from2010). It includes the P surplus on agricultural and non-agricultural areas. Details in Section 3.4.	Batool et al. 2024
Npoint_Pop_fr om1991, Npoint_Pop_fr om2010	kg N ha ⁻¹ y ⁻¹	Mean annual nitrogen (N) input from point sources with the population disaggregated approach during the period 1991-2021 (from1991) and 2010-2021 (from2010).	Sarrazin et al. 2024
Ppoint_Pop_fro m1991, Ppoint_Pop_fro m2010	kg N ha ⁻¹ y ⁻¹	Mean annual phosphorus (P) input from point sources with the population disaggregated approach during the period 1991-2021 (from1991) and 2010-2021 (from2010).	Sarrazin et al. 2024
Npoint_WWTP _from1991, Npoint_WWTP _from2010	kg N ha ⁻¹ y ⁻¹	Mean annual nitrogen (N) input with the wastewater treatment plant disaggregated approach during the period 1991-2021 (from1991) and 2010-2021 (from2010).	Sarrazin et al. 2024
Ppoint_WWTP _from1991, Ppoint_WWTP _from2010	kg N ha ⁻¹ y ⁻¹	Mean annual phosphorus (P) input from point sources with the wastewater treatment plant disaggregated approach during the period 1991-2021 (from1991) and 2010-2021 (from2010).	Sarrazin et al. 2024
f_Npoint_Pop_ from1991, f_Npoint_Pop_ from2010	kg N ha ⁻¹ y ⁻¹	Fraction of point source loads from total N input loads based on the population disaggregated point source data (Npoint_Pop) during the period 1991-2021 (from1991) and 2010-2021 (from2010). $f_{N_{point}} = N_{point} / (N_{point} + N_{surp_{Haussermann}})$	
f_Npoint_WW TP_from1991, f_Npoint_WW TP_from2010	kg N ha ⁻¹ y ⁻¹	Fraction of point source loads from total N input loads based on the WWTP disaggregated point source data (Npoint_Pop) during the period 1991-2021 (from1991) and 2010-2021 (from2010).	
N_T_YKM2	t N km ⁻² y ⁻¹	Mean N input from point sources summing all N emission values provided in the EU domestic waste emissions data base	Vigiak et al. (2019); Vigiak et al. (2020)
P_T_YKM2	t P km ⁻² y ⁻¹	Mean P input from point sources summing all P emission values provided in the EU domestic waste emissions data base	Vigiak et al. (2019); Vigiak et al. (2020)
BOD_T_YKM 2	t O km ⁻² y ⁻¹	Mean five-days biochemical oxygen demand (BOD) input from point sources summing all BOD emission values provided in the EU domestic waste emissions data base	Vigiak et al. (2019); Vigiak et al. (2020)
N_T_YEW	t N inh ⁻¹ y ⁻¹	Calculated N input per person (from EU domestic waste emissions data base)	Vigiak et al. (2019); Vigiak et al. (2020)

			$N_T_YEW = N_T_YKM2 / nEW * Area_km2$	
P_T_YEW	$t P \text{ inh}^{-1} \text{ y}^{-1}$	Calculated P input per person (from EU domestic waste emissions data base) $P_T_YEW = P_T_YKM2 / nEW * Area_km2$	Vigiak et al. (2019); Vigiak et al. (2020)	
nEW	-	Calculated number of inhabitants, $nEW = pdens * Area_km2$	<i>CIESIN (2017)</i>	
n_UWWTP	-	Number of point sources from European data base (UWWTP data base)	EEA (2017)	
f_sarea	-	Fraction of source area in the catchment. Source areas were defined as seasonal, perennial cropland and grassland land cover classes using a highly resolved land use map (Pflugmacher et al., 2018)	Source areas based on Pflugmacher et al. (2018)	
het_h	m^{-1}	Slope of relative frequency of source areas in classes of flow distances to stream as a proxy for horizontal source heterogeneity. For details refer to Ebeling, Kumar, et al. (2021)	Source areas based on Pflugmacher et al. (2018)	
R2_het_h	-	Coefficient of determination of horizontal source heterogeneity het_h		
sdist_mean	m	Mean lateral flow distance of source areas to stream. For details refer to Ebeling, Kumar, et al. (2021)	Source areas based on Pflugmacher et al. (2018)	
het_v	-	Mean ratio between potential seepage and groundwater $\text{NO}_3\text{-N}$ concentrations as proxy for vertical concentration heterogeneity. For details refer to Ebeling, Kumar, et al. (2021)	Knoll et al. (2020)	
P_available_agri	kg ha^{-1}	Available P stock in the agricultural topsoil (0-20 cm)	Panagos et al. (2022)	
P_available		Available P stock from agricultural topsoil scaled to the whole catchment area, i.e. $P_{available_agri}$ is scaled by the fraction of agriculture (f_{agric})	Panagos et al. (2022), EEA (2016)	
Lithology and soils	f_calc	-	Fraction of calcareous rocks (Lithology level 4)	BGR & UNESCO (eds.) (2014)
	f_calc_sed	-	Fraction of calcareous rocks and sediments (Lithology level 4, coarse and fine sediments aggregated)	BGR & UNESCO (eds.) (2014)
	f_magma	-	Fraction of magmatic rocks (Lithology level 4)	BGR & UNESCO (eds.) (2014)
	f_metam	-	Fraction of metamorphic rocks (Lithology level 4)	BGR & UNESCO (eds.) (2014)

f_sedim	-	Fraction of sedimentary aquifer (Lithology level 4, coarse and fine sediments aggregated)	BGR & UNESCO (eds.) (2014)
f_silic	-	Fraction of siliciclastic rocks (Lithology level 4)	BGR & UNESCO (eds.) (2014)
f_sili_sed	-	Fraction of siliciclastic rocks and sediments (Lithology level 4, coarse and fine sediments aggregated)	BGR & UNESCO (eds.) (2014)
f_consol	-	Fraction of consolidated rocks (Lithology Level 5)	BGR & UNESCO (eds.) (2014)
f_part_consol	-	Fraction of partly consolidated rocks (Lithology Level 5)	BGR & UNESCO (eds.) (2014)
f_unconsol	-	Fraction of unconsolidated rocks (Lithology Level 5)	BGR & UNESCO (eds.) (2014)
f_porous	-	Fraction of porous aquifer (code 1 and 2 of aquifer type)	BGR & UNESCO (eds.) (2014)
f_porous1	-	Fraction of porous aquifer (code 1 of aquifer type)	BGR & UNESCO (eds.) (2014)
f_porous2	-	Fraction of porous aquifer (code 2 of aquifer type)	BGR & UNESCO (eds.) (2014)
f_fissured	-	Fraction of fissured aquifer (code 3 and 4 of aquifer type)	BGR & UNESCO (eds.) (2014)
f_fiss1	-	Fraction of fissured aquifer (code 3 of aquifer type)	BGR & UNESCO (eds.) (2014)
f_fiss2	-	Fraction of fissured aquifer (code 4 of aquifer type)	BGR & UNESCO (eds.) (2014)
f_hard	-	Fraction of locally aquiferous and non-aquiferous aquifer (code 5 and 6 of aquifer type)	BGR & UNESCO (eds.) (2014)
f_hard1	-	Fraction of locally aquiferous rocks (code 5 of aquifer type)	BGR & UNESCO (eds.) (2014)
f_hard2	-	Fraction of non-aquiferous rocks (code 6 of aquifer type)	BGR & UNESCO (eds.) (2014)
f_inwater	-	Fraction of inland water (code 200 of aquifer type)	BGR & UNESCO (eds.) (2014)
f_ice	-	Fraction of snow or ice field (code 300 of aquifer type)	BGR & UNESCO (eds.) (2014)
dtb.median	cm	Median depth to bedrock in the catchment	Shangguan et al. (2017)
f_gwsoils	-	Fraction of water-impacted soils in the catchment (from soil map 1:250,000), including	BGR (2018)

			stagnosols, semi-terrestrial, semi-subhydric, subhydric and moor soils	
f_sand	-		Mean fraction of sand in soil horizons of the top 100 cm	FAO/IIASA/ISRIC/ISSCAS/JRC (2012)
f_silt			Mean fraction of silt in soil horizons of the top 100 cm	
f_clay			Mean fraction of clay in soil horizons of the top 100 cm	
f_clay_agri			Mean fraction of clay in soil horizons of the top 100 cm on agricultural land use (Class 2 Level 1 CORINE; see f_clay and f_agric)	FAO/IIASA/ISRIC/ISSCAS/JRC (2012), EEA (2016a)
WaterRoots	mm		Mean available water content in the root zone from pedo-transfer functions	Livneh et al. (2015); Samaniego et al. (2010); Zink et al. (2017)
thetaS	-		Mean porosity in catchment from pedo-transfer functions	Livneh et al. (2015); Samaniego et al. (2010); Zink et al. (2017)
soilN.mean	g kg ⁻¹		Mean top soil N in catchment	Ballabio et al. (2019)
soilP.mean	mg kg ⁻¹		Mean top soil P in catchment	Ballabio et al. (2019)
soilCN.mean	-		Mean top soil C/N ratio in catchment	Ballabio et al. (2019)
soilpH_CaCl	-		Mean top soil pH from CaCl ₂ 0.01 M solution in the catchment	Ballabio et al. (2019)
soilpH_H2O	-		Mean top soil pH measured in water in the catchment	Ballabio et al. (2019)
Hydrology	Q_StartDate	YYYY-MM-DD	Starting date of Q time series used for calculating hydrological indices (from November 1990, if possible and at least 3 years of data (all 637 stations fulfilled that))	
	Q_EndDate	YYYY-MM-DD	End date of Q time series used for calculating hydrological indices (up to October 2020 if available)	
	Q_gaps	boolean	If there are missing discharge values (a gap) in between Q_StartDate and Q_EndDate, the value is 1; without any gap the value is 0.	
	Q_nNAs	-	Number of missing values in between Q_StartDate and Q_EndDate.	
	Q_mean	m ³ s ⁻¹	Mean discharge (data for the period Q_StartDate-Q_EndDate)	
	Q_median	m ³ s ⁻¹	Median discharge (data for the period Q_StartDate-Q_EndDate)	

Q_spec	mm y ⁻¹	Mean annual specific discharge (data for the period Q_StartDate-Q_EndDate)	
Q_CVQ	-	Coefficient of variation of time series of daily Q (data for the period Q_StartDate-Q_EndDate)	
Q_medSum	m ³ s ⁻¹	Median summer discharge (months May-October) (data for the period Q_StartDate-Q_EndDate)	
Q_medWin	m ³ s ⁻¹	Median winter discharge (months November-April) (data for the period Q_StartDate-Q_EndDate)	
Q_Sum2Win	-	Seasonality index of Q, as ratio between median summer and median winter Q (data for the period Q_StartDate-Q_EndDate)	
BFI	-	Base flow index calculated according to WMO [2008] with <i>lfsstat</i> package (version 0.9.4) in R (data for the period Q_StartDate-Q_EndDate)	
flashi	-	Flashiness index of Q as the ratio between 5 % percentile and 95 % percentile of Q time series (data for the period Q_StartDate-Q_EndDate)	
Climate	P_mm	mm y ⁻¹	Mean annual precipitation (period 1986-2015) Cornes et al. (2018)
	P_SIsw	-	Seasonality of precipitation as the ratio between mean summer (Jun-Aug) and winter (Dec-Feb) precipitation (period 1986-2015) Cornes et al. (2018)
	P_SI	-	Seasonality index of precipitation as the mean difference between monthly averages of daily precipitation and year average of daily precipitation (period 1986-2015) Cornes et al. (2018)
	P_lambda	d ⁻¹	Mean precipitation frequency λ as used by Botter et al. (2013) with rain days for precipitation above 1 mm (period 1986-2015) Cornes et al. (2018)
	P_alpha	mm d ⁻¹	Mean precipitation depth as used by Botter et al. (2013) with rain days for precipitation above 1 mm (period 1986-2015) Cornes et al. (2018)
	PET_mm	mm y ⁻¹	Mean annual potential evapotranspiration (period 1986-2015) Cornes et al. (2018)
AI	-	Aridity index as AI=PET_mm/P_mm (period 1986-2015) Cornes et al. (2018)	
T_mean	°C	Mean annual air temperature (period 1986-2015) Cornes et al. (2018)	

478 The study was conceptualized by PE, AM, and RK. PE played a key role in data management, ensuring
479 the quality, homogenization, and preprocessing of the data, as well as developing the methodology for
480 matching and merging CAMELS/Caravan discharge data. PE also prepared the results, created
481 visualizations, wrote the first draft of the manuscript and revised the manuscript. AW, US collected the
482 water quality and quantity data from federal authorities and together with AH contributed to data quality
483 control. SH, TN contributed to matching and merging QUADICA-CAMELS and Caravan stations, SH
484 additionally extracted some new catchment attributes. Additionally, TN developed a Shiny App to
485 facilitate data exploration in the data repository, with additions from PE. MB, FS, RK provided the
486 catchment N and P input data. RK also contributed the climate and LAI data.

487

488 **Competing interests.** The authors declare that they have no conflict of interest.

489

490 **Acknowledgements.** We gratefully thank all data collectors, processors and providers including the
491 federal state environmental agencies and all other contributors to this data set. We thank Nils Turner for
492 his contributions to water quality data control, José Ledesma for discussions on the quality of discharge
493 data, Sabine Attinger and Jan H. Fleckenstein for their initial input to QUADICA v1, Linus Schauer for
494 providing the Strahler order as catchment descriptor, and Nicoletta Leitgeb for providing up- and
495 downstream stations. We gratefully acknowledge Martin Bach and Uwe Häußermann, Justus-Liebig-
496 University of Giessen, for the provision of the two data sets on the agricultural N surplus data for
497 Germany. We acknowledge the E-OBS data set from the EU-FP6 project UERRA (<http://www.uerra.eu>)
498 and the Copernicus Climate Change Service, and the data providers in the ECA&D project
499 (<https://www.ecad.eu>). The authors additionally acknowledge several organizations for the data products
500 used here, including the BfG, BGR, SGD, EEA, FAO, IIASA, ISRIC, ISSCAS, and JRC. Large Language
501 Models (LLM), in particular Llama3 405 embedded in the Helmholtz AI Jülich service Blablador, have
502 been used to increase readability of parts of the text - we thank the providers.

References

504 Addor, N., Newman, A. J., Mizukami, N., and Clark, M. P.: The CAMELS data set: catchment attributes
 505 and meteorology for large-sample studies, *Hydrol Earth Syst Sc*, 21, 5293-5313,
 506 <https://doi.org/10.5194/hess-21-5293-2017>, 2017.

507 Alvarez-Garreton, C., Mendoza, P. A., Boisier, J. P., Addor, N., Galleguillos, M., Zambrano-Bigiarini,
 508 M., Lara, A., Puelma, C., Cortes, G., Garreaud, R., McPhee, J., and Ayala, A.: The CAMELS-CL dataset:
 509 catchment attributes and meteorology for large sample studies – Chile dataset, *Hydrol Earth Syst Sc*, 22,
 510 5817-5846, <https://doi.org/10.5194/hess-22-5817-2018>, 2018.

511 Ballabio, C., Lugato, E., Fernández-Ugalde, O., Orgiazzi, A., Jones, A., Borrelli, P., Montanarella, L.,
 512 and Panagos, P.: Mapping LUCAS topsoil chemical properties at European scale using Gaussian process
 513 regression, *Geoderma*, 355, 113912, <https://doi.org/10.1016/j.geoderma.2019.113912>, 2019.

514 Batool, M., Sarrazin, F. J., and Kumar, R.: Century-long reconstruction of gridded phosphorus surplus
 515 across Europe (1850–2019), *Earth System Science Data*, 17, 881-916, 10.5194/essd-17-881-2025, 2025.

516 Batool, M., Sarrazin, F. J., Attinger, S., Basu, N. B., Van Meter, K., and Kumar, R.: Long-term annual
 517 soil nitrogen surplus across Europe (1850–2019), *Scientific Data*, 9, 612, 10.1038/s41597-022-01693-9,
 518 2022.

519 Behrendt, H., Bach, M., Kunkel, R., Opitz, D., Pagenkopf, W.-G., Scholz, G., and Wendland, F.: Nutrient
 520 Emissions into River Basins of Germany on the Basis of a Harmonized Procedure, UBA-Texte,
 521 82/03, 2003.

522 Chagas, V. B. P., Chaffe, P. L. B., Addor, N., Fan, F. M., Fleischmann, A. S., Paiva, R. C. D., and Siqueira,
 523 V. A.: CAMELS-BR: hydrometeorological time series and landscape attributes for 897 catchments in
 524 Brazil, *Earth Syst. Sci. Data*, 12, 2075-2096, <https://doi.org/10.5194/essd-12-2075-2020>, 2020.

525 Cornes, R. C., van der Schrier, G., van den Besselaar, E. J. M., and Jones, P. D.: An Ensemble Version
 526 of the E-OBS Temperature and Precipitation Data Sets, *Journal of Geophysical Research: Atmospheres*,
 527 123, 9391-9409, <https://doi.org/10.1029/2017jd028200>, 2018.

528 Coxon, G., Addor, N., Bloomfield, J. P., Freer, J., Fry, M., Hannaford, J., Howden, N. J. K., Lane, R.,
 529 Lewis, M., Robinson, E. L., Wagener, T., and Woods, R.: CAMELS-GB: hydrometeorological time series
 530 and landscape attributes for 671 catchments in Great Britain, *Earth Syst. Sci. Data*, 12, 2459-2483,
 531 <https://doi.org/10.5194/essd-12-2459-2020>, 2020.

532 De Jager, A. and Vogt, J.: Rivers and Catchments of Europe - Catchment Characterisation Model (CCM)
 533 (2.1), European Commission, Joint Research Centre (JRC) [dataset], 2007.

534 do Nascimento, T. V. M., Höge, M., Schönenberger, U., Pool, S., Siber, R., Kauzlaric, M., Staudinger,
 535 M., Horton, P., Floriancic, M. G., Storck, F. R., Rinta, P., Seibert, J., and Fenicia, F.: Swiss data quality:
 536 augmenting CAMELS-CH with isotopes, water quality, agricultural and atmospheric data, *Scientific*
 537 *Data*, 12, 1283, 10.1038/s41597-025-05625-1, 2025.

538 Dolich, A., Maharjan, A., Mälicke, M., Manoj J. A., and Loritz, R.: Caravan-DE: Caravan extension
 539 Germany - German dataset for large-sample hydrology (v1.0.1) [dataset],
 540 <https://doi.org/10.5281/zenodo.13983616>, 2024.

541 Dupas, R., Lintern, A., Musolff, A., Winter, C., Fovet, O., and Durand, P.: Water quality responses to
 542 hydrological droughts can be predicted from long-term concentration–discharge relationships,
 543 *Environmental Research: Water*, 1, 10.1088/3033-4942/adb906, 2025.

544 E-OBS: (v18.0) [dataset], 2018.
545 Ebeling, P., Kumar, R., Weber, M., Knoll, L., Fleckenstein, J. H., and Musolff, A.: Archetypes and
546 Controls of Riverine Nutrient Export Across German Catchments, *Water Resour Res*, 57,
547 e2020WR028134, <https://doi.org/10.1029/2020WR028134>, 2021a.
548 Ebeling, P., Dupas, R., Abbott, B., Kumar, R., Ehrhardt, S., Fleckenstein, J. H., and Musolff, A.: Long-
549 Term Nitrate Trajectories Vary by Season in Western European Catchments, *Global Biogeochemical*
550 *Cycles*, 35, e2021GB007050, <https://doi.org/10.1029/2021GB007050>, 2021b.
551 Ebeling, P., Kumar, R., Lutz, S. R., Nguyen, T., Sarrazin, F., Weber, M., Büttner, O., Attinger, S., and
552 Musolff, A.: QUADICA: water QUAlity, DIcharge and Catchment Attributes for large-sample studies
553 in Germany, *Earth Syst. Sci. Data*, 14, 3715-3741, 10.5194/essd-14-3715-2022, 2022.
554 Ebeling, P., Kumar, R., Musolff, A., Nguyen, T., Hubig, A., Haug, S., Scharfenberger, U., Batool, M.,
555 Wachholz, A., and Sarrazin, F.: QUADICA v2 - water quality, discharge and catchment attributes for
556 large-sample studies in Germany, *HydroShare* [dataset],
557 <https://doi.org/10.4211/hs.c2866cd416b94ca386deb5758834311f>, 2025.
558 EC: Council Directive 91/676/EEC of 12 December 1991 concerning the protection of waters against
559 pollution caused by nitrates from agricultural sources, *Official Journal of the European Communities*,
560 1991.
561 EEA: CORINE Land Cover 2012 v18.5, European Environment Agency [dataset], 2016.
562 EEA: CORINE Land Cover 2018 (raster 100 m), Europe, 6-yearly - version 2020_20u1, May 2020
563 European Environment Agency [dataset], 10.2909/960998c1-1870-4e82-8051-6485205ebbac, 2019.
564 EEA: EU-Hydro River Network Database 2006-2012 (vector), Europe - version 1.3 (version 1.3),
565 European Environment Agency (EEA). Copernicus Land Monitoring Service [dataset],
566 10.2909/393359a7-7ebd-4a52-80ac-1a18d5f3db9c, 2020.
567 Ehrhardt, S., Ebeling, P., Dupas, R., Kumar, R., Fleckenstein, J. H., and Musolff, A.: Nitrate Transport
568 and Retention in Western European Catchments Are Shaped by Hydroclimate and Subsurface Properties,
569 *Water Resour Res*, 57, e2020WR029469, <https://doi.org/10.1029/2020WR029469>, 2021.
570 Fernandez, N., Cohen, M. J., and Jawitz, J. W.: ChemLotUS: A Benchmark Data Set of Lotic Chemistry
571 Across US River Networks, *Water Resour Res*, 61, e2024WR039355,
572 <https://doi.org/10.1029/2024WR039355>, 2025.
573 Fowler, K. J. A., Acharya, S. C., Addor, N., Chou, C., and Peel, M. C.: CAMELS-AUS:
574 hydrometeorological time series and landscape attributes for 222 catchments in Australia, *Earth Syst. Sci.*
575 *Data*, 13, 3847-3867, <https://doi.org/10.5194/essd-13-3847-2021>, 2021.
576 Gupta, H. V., Perrin, C., Blöschl, G., Montanari, A., Kumar, R., Clark, M., and Andréassian, V.: Large-
577 sample hydrology: a need to balance depth with breadth, *Hydrol. Earth Syst. Sci.*, 18, 463-477,
578 <https://doi.org/10.5194/hess-18-463-2014>, 2014.
579 Häußermann, U., Klement, L., Breuer, L., Ullrich, A., Wechsung, G., and Bach, M.: Nitrogen soil surface
580 budgets for districts in Germany 1995 to 2017, *Environmental Sciences Europe*, 32, 109, 10.1186/s12302-
581 020-00382-x, 2020.
582 Heudorfer, B., Gupta, H. V., and Loritz, R.: Are Deep Learning Models in Hydrology Entity Aware?,
583 *Geophysical Research Letters*, 52, 10.1029/2024gl113036, 2025.

584 Hirsch, R. M. and De Cicco, L. A.: User Guide to Exploration and Graphics for RivEr Trends (EGRET)
585 and dataRetrieval: R Packages for Hydrologic Data, U.S. Geological Survey Techniques and Methods
586 book 4, chap. A10, 93, <https://dx.doi.org/10.3133/tm4A10>, 2015.

587 Hirsch, R. M., Moyer, D. L., and Archfield, S. A.: Weighted Regressions on Time, Discharge, and Season
588 (WRTDS), with an Application to Chesapeake Bay River Inputs, JAWRA Journal of the American Water
589 Resources Association, 46, 857-880, <https://doi.org/10.1111/j.1752-1688.2010.00482.x>, 2010.

590 Kratzert, F., Klotz, D., Brenner, C., Schulz, K., and Herrnegger, M.: Rainfall–runoff modelling using
591 Long Short-Term Memory (LSTM) networks, Hydrol Earth Syst Sc, 22, 6005-6022, 10.5194/hess-22-
592 6005-2018, 2018.

593 Kratzert, F., Nearing, G., Addor, N., Erickson, T., Gauch, M., Gilon, O., Gudmundsson, L., Hassidim,
594 A., Klotz, D., Nevo, S., Shalev, G., and Matias, Y.: Caravan - A global community dataset for large-
595 sample hydrology, Scientific Data, 10, 61, 10.1038/s41597-023-01975-w, 2023.

596 Loritz, R., Dolich, A., Acuña Espinoza, E., Ebeling, P., Guse, B., Götte, J., Hassler, S. K., Hauffe, C.,
597 Heidbüchel, I., Kiesel, J., Mälicke, M., Müller-Thomy, H., Stölzle, M., and Tarasova, L.: CAMELS-DE:
598 hydro-meteorological time series and attributes for 1582 catchments in Germany, Earth Syst. Sci. Data,
599 16, 5625-5642, 10.5194/essd-16-5625-2024, 2024.

600 Minasny, B., McBratney, A. B., Brough, D. M., and Jacquier, D.: Models relating soil pH measurements
601 in water and calcium chloride that incorporate electrolyte concentration, European Journal of Soil
602 Science, 62, 728-732, 10.1111/j.1365-2389.2011.01386.x, 2011.

603 Minaudo, C., Abonyi, A., Alcaraz, C., Diamond, J., Howden, N. J. K., Rode, M., Romero, E., Thieu, V.,
604 Worrall, F., Zhang, Q., and Benito, X.: OLIGOTREND, a global database of multi-decadal chlorophyll a
605 and water quality time series for rivers, lakes, and estuaries, Earth System Science Data, 17, 3411-3430,
606 10.5194/essd-17-3411-2025, 2025.

607 Musolff, A.: WQQDB - water quality and quantity data base Germany: metadata, HydroShare [dataset],
608 <https://doi.org/10.4211/hs.a42addcbd59a466a9aa56472dfef8721>, 2020.

609 Musolff, A., Grau, T., Weber, M., Ebeling, P., Samaniego-Eguiguren, L., and Kumar, R.: WQQDB: water
610 quality and quantity data base Germany [dataset], 2020.

611 Nguyen, T. V., Sarrazin, F. J., Ebeling, P., Musolff, A., Fleckenstein, J. H., and Kumar, R.: Toward
612 Understanding of Long-Term Nitrogen Transport and Retention Dynamics Across German Catchments,
613 Geophysical Research Letters, 49, e2022GL100278, <https://doi.org/10.1029/2022GL100278>, 2022.

614 Panagos, P., Königner, J., Ballabio, C., Liakos, L., Muntwyler, A., Borrelli, P., and Lugato, E.:
615 Improving the phosphorus budget of European agricultural soils, Science of The Total Environment, 853,
616 158706, <https://doi.org/10.1016/j.scitotenv.2022.158706>, 2022.

617 Rakovec, O., Samaniego, L., Hari, V., Markonis, Y., Moravec, V., Thober, S., Hanel, M., and Kumar, R.:
618 The 2018–2020 Multi-Year Drought Sets a New Benchmark in Europe, Earth's Future, 10,
619 e2021EF002394, 10.1029/2021EF002394, 2022.

620 Saavedra, F., Musolff, A., von Freyberg, J., Merz, R., Basso, S., and Tarasova, L.: Disentangling scatter
621 in long-term concentration–discharge relationships: the role of event types, Hydrol Earth Syst Sc, 26,
622 6227-6245, 10.5194/hess-26-6227-2022, 2022.

623 Saavedra, F., Musolff, A., Von Freyberg, J., Merz, R., Knöller, K., Müller, C., Brunner, M., and Tarasova,
624 L.: Winter post-droughts amplify extreme nitrate concentrations in German rivers, Environmental
625 Research Letters, 19, 024007, 10.1088/1748-9326/ad19ed, 2024.

626 Saha, G. K., Rahmani, F., Shen, C., Li, L., and Cibin, R.: A deep learning-based novel approach to
627 generate continuous daily stream nitrate concentration for nitrate data-sparse watersheds, *Sci Total*
628 *Environ*, 878, 162930, 10.1016/j.scitotenv.2023.162930, 2023.

629 Sarrazin, F. J., Attinger, S., and Kumar, R.: Gridded dataset of nitrogen and phosphorus point sources
630 from wastewater in Germany (1950-2019), *Earth Syst. Sci. Data Discuss.*, 2024, 1-54, 10.5194/essd-
631 2023-474, 2024.

632 Sarrazin, F. J., Kumar, R., Basu, N. B., Musolff, A., Weber, M., Van Meter, K. J., and Attinger, S.:
633 Characterizing Catchment-Scale Nitrogen Legacies and Constraining Their Uncertainties, *Water Resour*
634 *Res*, 58, e2021WR031587, <https://doi.org/10.1029/2021WR031587>, 2022.

635 Sterle, G., Perdrial, J., Kincaid, D. W., Underwood, K. L., Rizzo, D. M., Haq, I. U., Li, L., Lee, B. S.,
636 Adler, T., Wen, H., Middleton, H., and Harpold, A. A.: CAMELS-Chem: augmenting CAMELS
637 (Catchment Attributes and Meteorology for Large-sample Studies) with atmospheric and stream water
638 chemistry data, *Hydrol. Earth Syst. Sci.*, 28, 611-630, 10.5194/hess-28-611-2024, 2024.

639 Van Meter, K. J. and Basu, N. B.: Catchment legacies and time lags: a parsimonious watershed model to
640 predict the effects of legacy storage on nitrogen export, *PLoS One*, 10, e0125971,
641 10.1371/journal.pone.0125971, 2015.

642 Virro, H., Amatulli, G., Kmoch, A., Shen, L., and Uuemaa, E.: GRQA: Global River Water Quality
643 Archive, *Earth Syst. Sci. Data*, 13, 5483-5507, 10.5194/essd-13-5483-2021, 2021.

644 Wachholz, A., Dehaspe, J., Ebeling, P., Kumar, R., Musolff, A., Saavedra, F., Winter, C., Yang, S., and
645 Graeber, D.: Stoichiometry on the edge - Humans induce strong imbalances of reactive C:N:P ratios in
646 streams, *Environmental Research Letters*, 18, 044016, 10.1088/1748-9326/acc3b1, 2023.

647 Winter, C., Nguyen, T. V., Musolff, A., Lutz, S. R., Rode, M., Kumar, R., and Fleckenstein, J. H.:
648 Droughts can reduce the nitrogen retention capacity of catchments, *Hydrol. Earth Syst. Sci.*, 27, 303-318,
649 10.5194/hess-27-303-2023, 2023.

650 Yan, K., Wang, J., Peng, R., Yang, K., Chen, X., Yin, G., Dong, J., Weiss, M., Pu, J., and Myneni, R. B.:
651 HiQ-LAI: a high-quality reprocessed MODIS leaf area index dataset with better spatiotemporal
652 consistency from 2000 to 2022, *Earth Syst. Sci. Data*, 16, 1601-1622, 10.5194/essd-16-1601-2024, 2024.

653 Zarei, E., Noori, R., Jun, C., Bateni, S. M., Kianmehr, P., and Zhu, S.: A Comprehensive Water Chemistry
654 Dataset for Iranian Rivers, *Scientific Data*, 12, 1646, 10.1038/s41597-025-05932-7, 2025.

655 Zhi, W., Ouyang, W., Shen, C., and Li, L.: Temperature outweighs light and flow as the predominant
656 driver of dissolved oxygen in US rivers, *Nature Water*, 1, 249-260, 10.1038/s44221-023-00038-z, 2023.

657 Zhi, W., Feng, D., Tsai, W.-P., Sterle, G., Harpold, A., Shen, C., and Li, L.: From Hydrometeorology to
658 River Water Quality: Can a Deep Learning Model Predict Dissolved Oxygen at the Continental Scale?,
659 *Environmental Science & Technology*, 55, 2357-2368, 10.1021/acs.est.0c06783, 2021.

660